

A new five unknown quasi-3D type HSDT for thermomechanical bending analysis of FGM sandwich plates

Abdeldjalil Benbakhti¹, Mohamed Bachir Bouiadjra^{*2},
Nouredine Retiel¹ and Abdelouahed Tounsi³

¹ *Faculté des Sciences et de la Technologie, Département de Génie Mécanique,
University Abdelhamid Ibn Badis, Mostaganem, 27000, Algérie*

² *Laboratoire des Structures et Matériaux Avancés dans le Génie Civil et Travaux Publics,
Université de Sidi Bel Abbès, Faculté de Technologie, Département de génie civil, Algeria*

³ *Material and Hydrology Laboratory, University of Sidi Bel Abbès, Faculty of Technology,
Civil Engineering Department, Algeria*

(Received February 15, 2016, Revised October 11, 2016, Accepted November 03, 2016)

Abstract. This work investigates a thermomechanical bending analysis of functionally graded sandwich plates by proposing a novel quasi-3D type higher order shear deformation theory (HSDT). The mathematical model introduces only 5 variables as the first order shear deformation theory (FSDT). Unlike the conventional HSDT, the present one presents a novel displacement field which includes undetermined integral variables. The mechanical properties of functionally graded layers of the plate are supposed to change in the thickness direction according to a power law distribution. The core layer is still homogeneous and made of an isotropic ceramic material. The governing equations for the thermomechanical bending investigation are obtained through the principle of virtual work and solved via Navier-type method. Interesting results are determined and compared with quasi-3D and 2D HSDTs. The influences of functionally graded material (FGM) layer thickness, power law index, layer thickness ratio, thickness ratio and aspect ratio on the deflections and stresses of functionally graded sandwich plates are discussed.

Keywords: sandwich plate; thermomechanical; analytical modeling; functionally graded material; stretching effect

1. Introduction

Plates made of functionally graded material (FGM) are widely employed in various branches of engineering such as mechanical, aerospace, chemical, electrical etc. The advantages of FGM structures present high thermal resistance and graded change of material characteristics along the chosen direction. For designing FGM plates for application in high temperature environment, thermomechanical stresses and deflections are important parameters to be considered. The present article deals with developing a new quasi-3D type HSDT to study the thermomechanical static response of FGM sandwich plates. The published works related to the field of thermal and mechanical bending of FGM plates are indicated and discussed in the following few paragraphs.

*Corresponding author, Professor, E-mail: mohamedbachirbouiadjra@gmail.com

Shariyat (2010) proposed a linear and nonlinear bending investigation of sandwich plate under thermomechanical loads based on generalized 3D high-order double superposition global–local theory, respectively. Xiang *et al.* (2009) discussed the bending behavior of sandwich plates subjected to mechanical loads by using several HSDTs. Reddy and Cheng (2001) presented a 3D model for a FG plate subjected to mechanical and thermal loads, both applied at the top of the FG plate. Cetkovic and Vuksanovic (2000) employed a generalized layerwise model to investigate the sandwich plates under mechanical loads. This model considers transverse variation of the in-plane displacement components in terms of 1D linear Lagrangian finite elements. Natarajan and Manickam (2012) used a C^0 8-noded quadrilateral plate element with 13 degrees of freedom per node based on a HSDT to examine the bending response of FG sandwich plates. Grover *et al.* (2013) proposed a novel inverse hyperbolic shear deformation theory for the bending and buckling behavior of sandwich plates considering a displacement field with 5 variables without thickness stretching effect. Golmakani (2013) investigated the nonlinear deflection analysis of FG solid and hollow rotating axisymmetric disk with uniform and variable thickness under thermal and mechanical loads. Ait Amar Meziane *et al.* (2014) proposed an efficient refined shear deformation theory to analyze the vibration and the buckling behavior of exponentially graded sandwich plate resting on elastic foundation under different support conditions. Houari *et al.* (2013) studied the FG sandwich plates under thermal load by employing a HSDT with thickness stretching influence. Matsunaga (2009) modeled the displacement field with power series of the thickness coordinate for the investigation of FG plates subjected to thermal and mechanical loads based on 2D HSDT. Talha and Singh (2011) analyzed thermomechanical induced vibration properties of FG plates based on modified HSDT. Tounsi *et al.* (2013) proposed a bending analysis of sandwich plates with FG core based on refined HSDT. Boudarba *et al.* (2013) analyzed the thermomechanical static response of FGM thick plates resting on Winkler–Pasternak elastic foundations. Saidi *et al.* (2013) studied the thermomechanical bending response of FG sandwich plates considering a displacement field having 6 variables with thickness stretching effect. Sobhy (2013) analyzed the stability and dynamic response of exponentially graded sandwich plates resting on elastic foundations under various boundary conditions. Zidi *et al.* (2014) presented a static analysis of FG plates under hygro-thermo-mechanical loading using a four variable refined plate theory. Mahi *et al.* (2015) developed a novel hyperbolic shear deformation theory for bending and free vibration analysis of isotropic, functionally graded, sandwich and laminated composite plates. Hamidi *et al.* (2015) proposed a sinusoidal plate theory with 5-variables and stretching effect for thermomechanical bending of FG sandwich plates. Bouguenina *et al.* (2015) presented a numerical analysis of FG plates with variable thickness subjected to thermal buckling. Bouchafa *et al.* (2015) studied the thermal stresses and deflections of FG sandwich plates using a new refined hyperbolic shear deformation theory. Attia *et al.* (2015) studied the dynamic behavior of FG plates with temperature-dependent properties by employing various four variable refined plate theories. Kar and Panda (2015a) investigated the large deformation bending response of FG spherical shell using FEM. Kar and Panda (2015b) discussed the nonlinear flexural vibration of shear deformable FG spherical shell panel. Kar *et al.* (2015) studied the nonlinear flexural behavior of laminated composite flat panel under hygro-thermomechanical loading. Bennoun *et al.* (2016) proposed a new five variable refined plate theory for vibration analysis of FG sandwich plates. Recently, Kar and Panda (2016) studied the nonlinear thermomechanical deformation response of P-FGM shallow spherical shell panel. Also, Mehar and Panda (2016) contributed to a thermoelastic analysis of FG-CNT reinforced Shear deformable composite plate under various loadings. Kar and Panda (2016) studied nonlinear thermomechanical behavior of functionally graded material

cylindrical / hyperbolic / elliptical shell panel with temperature - dependent and temperature - independent properties. Sahoo *et al.* (2016a) developed a new model that treats static, free vibration and transient response of laminated composite curved shallow panel-an experimental approach. Mahapatra *et al.* (2016a) analyzed the nonlinear flexural analysis of laminated composite panel under hygro-thermo mechanical loading. Sahoo *et al.* (2016b) contributed to the nonlinear flexural analysis of shallow laminated carbon/epoxy composite curved shell panels. Sahoo *et al.* (2015) effectuated analyses for an experimental and numerical investigation of static and free vibration responses of woven glass/epoxy laminated composite plate. Mahapatra *et al.* (2016b) investigated the large amplitude bending behavior of laminated composite curved panels. Dutta *et al.* (2016) used a finite element approach for electro-magneto-elastic response of laminated composite plate. Singh *et al.* (2016) analyzed the nonlinear flexural response of single/doubly curved smart composite shell panels integrated with PFRC actuator. Ait Yahia *et al.* (2015) investigated the wave propagation in FG plates with porosities using various higher-order shear deformation plate theories. Bellifa *et al.* (2016) studied the bending and free vibration behavior of FG plates using a simple shear deformation theory and the concept the neutral surface position. Bounouara *et al.* (2016) presented a nonlocal zeroth-order shear deformation theory for free vibration of FG nanoscale plates resting on elastic foundation. Bourada *et al.* (2016) discussed the buckling response of isotropic and orthotropic plates using a novel four variable refined plate theory. Tounsi *et al.* (2016) presented a new 3-unknowns non-polynomial plate theory for buckling and vibration of FG sandwich plate. Also, Houari *et al.* (2016) proposed a new simple three-unknown sinusoidal shear deformation theory for FG plates.

On other hand, many HSDTs have been proposed over the last years for the investigation of structural elements. These models can be divided in two groups by a simple criterion: HSDTs with thickness stretching influence and HSDT without thickness stretching influence. When a model introduces the thickness stretching effect, the transverse displacement is assumed dependent by thickness coordinates obeying the Koiter's recommendation (1959), i.e., $\epsilon_z \neq 0$. In the literature many models that introduce thickness stretching influence to examine the bending, vibration and buckling response of FG single-layer and sandwich structures subjected to thermal α /and mechanical load can be found (Carrera *et al.* 2011, Bessaim *et al.* 2013, Belabed *et al.* 2014, Bousahla *et al.* 2014, Hebali *et al.* 2014, Bourada *et al.* 2015, Hamidi *et al.* 2015, Larbi Chaht *et al.* 2015).

This article proposes an analytical formulation of the thermomechanical static problem of FG sandwich plates by employing a novel quasi-3D type HSDT. The addition of the integral term in the displacement field leads to a reduction in the number of variables and governing equations. The sandwich plate faces are considered to have isotropic, two-constituent (metal-ceramic) material variation within the thickness, and the Young modulus, Poisson's ratio, and thermal expansion coefficient of the faces are supposed to change according to a power law variation in terms of the volume fractions of the constituents. The core layer remains homogeneous and fabricated by an isotropic ceramic material. The governing equations for the thermomechanical bending investigation are determined via the principle of virtual work. Navier-type analytical solutions are used for FG sandwich plates under thermomechanical load for simply supported boundary conditions. Numerical results for transverse displacements and stresses are examined. The influences of temperature field on the dimensionless in-plane and transverse shear stresses of the FG sandwich plate are investigated. The performance of the proposed model is checked by comparing results with other quasi-3D HSDTs and 2D HSDTs available in literature.

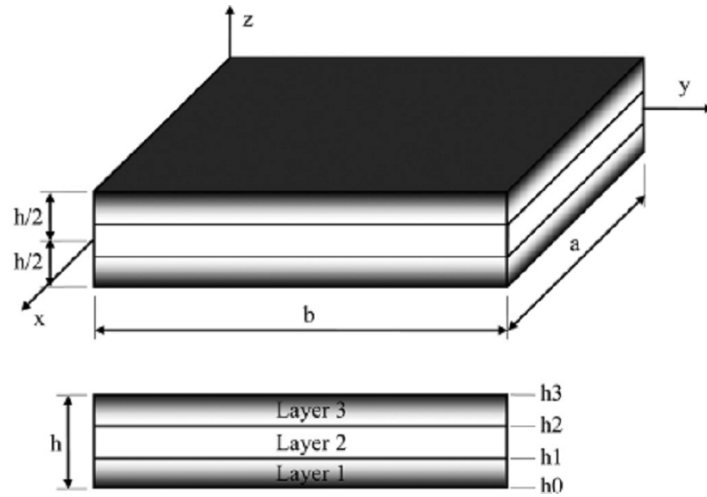


Fig. 1 Geometry and coordinates of rectangular FGM sandwich plate

2. Mathematical formulation

The mathematical model was constructed to solve a sandwich plate composed of three (metal-ceramic, ceramic, ceramic-metal) layers as shown in Fig. 1. The considered FG sandwich plate has as length a , width b and total thickness h . The rectangular Cartesian coordinate system x, y, z , has the surface $z = 0$, coinciding with the mid-surface of the plate. The face layers of the sandwich plate are composed by an isotropic material with material characteristics varying smoothly in the thickness direction only. The core layer is constituted by an isotropic homogeneous material. The vertical positions of the bottom surface, the two interfaces between the core and faces layers, and the top surface are defined, respectively, by $h_0 = -h / 2, h_1, h_2$ and $h_3 = h / 2$. The total thickness of the FG sandwich plate is h , where $h = t_c + t_{FGM}$ and $t_c = h_2 - h_1$. t_c and t_{FGM} are the layer thickness of the core and all-FGM layers, respectively.

The effective material characteristics for each layer, such as Young's modulus, Poisson's ratio and thermal expansion coefficient, can be defined as

$$P^{(n)}(z) = P_m + (P_c - P_m)V^{(n)} \tag{1}$$

where $P^{(n)}$ is the effective material characteristic of FGM of layer n . P_m and P_c defined the property of the bottom and top faces of layer 1 ($h_0 \leq z \leq h_1$), respectively, and vice versa for layer 3 ($h_2 \leq z \leq h_3$) depending on the volume fraction $V^{(n)}$ ($n = 1, 2, 3$). Note that P_m and P_c are, respectively, the corresponding characteristics of the metal and ceramic of the FG sandwich plate. The volume fraction v of the FGMs is supposed to obey a power-law function along the thickness direction (Saidi *et al.* 2013)

$$V^{(1)} = \left(\frac{z - h_0}{h_1 - h_0} \right)^k, \quad h_0 \leq z \leq h_1 \tag{2a}$$

$$V^{(2)} = 1, \quad h_1 \leq z \leq h_2 \tag{2b}$$

$$V^{(3)} = \left(\frac{z - h_3}{h_2 - h_3} \right)^k, \quad h_2 \leq z \leq h_3 \tag{2c}$$

where k is the gradient index, which takes values greater than or equals to zero. The core layer is independent of the value of k which is a fully ceramic layer.

2.1 Kinematic relations and constitutive relations

In this article, the conventional HSDTs with thickness stretching effect are modified by proposing some simplifying suppositions so that the number of unknowns is reduced. The displacement field of the existing HSDTs with thickness stretching effect is defined by

$$u(x, y, z) = u_0(x, y) - z \frac{\partial w_0}{\partial x} + f(z)\varphi_x(x, y) \tag{3a}$$

$$v(x, y, z) = v_0(x, y) - z \frac{\partial w_0}{\partial y} + f(z)\varphi_y(x, y) \tag{3b}$$

$$w(x, y, z) = w_0(x, y) + g(z)\varphi_z(x, y) \tag{3c}$$

where u_0 ; v_0 ; w_0 , φ_x , φ_y , and φ_z are six unknown displacements of the mid-plane of the plate, and $f(z)$ represents shape function defining the variation of the transverse shear strains and stresses across the thickness. In this article a novel displacement field with 5 unknowns is proposed

$$u(x, y, z) = u_0(x, y) - z \frac{\partial w_0}{\partial x} + k_1 f(z) \int \theta(x, y) dx \tag{4a}$$

$$v(x, y, z) = v_0(x, y) - z \frac{\partial w_0}{\partial y} + k_2 f(z) \int \theta(x, y) dy \tag{4b}$$

$$w(x, y, z) = w_0(x, y) + g(z)\varphi_z(x, y) \tag{4c}$$

The coefficients k_1 and k_2 depends on the geometry. In this article, the shape function is considered based on the hyperbolic function given by Nguyen (2015) as

$$f(z) = \sinh^{-1}\left(\frac{3z}{h}\right) - z \frac{6}{h\sqrt{13}} \quad \text{and} \quad g(z) = \frac{df(z)}{dz} \tag{5}$$

The linear strain relations obtained from the displacement model of Eqs. (4a)-(4c), valid for thin, moderately thick and thick plate under consideration are as follows

$$\begin{Bmatrix} \varepsilon_x \\ \varepsilon_y \\ \gamma_{xy} \end{Bmatrix} = \begin{Bmatrix} \varepsilon_x^0 \\ \varepsilon_y^0 \\ \gamma_{xy}^0 \end{Bmatrix} + z \begin{Bmatrix} k_x^b \\ k_y^b \\ k_{xy}^b \end{Bmatrix} + f(z) \begin{Bmatrix} k_x^s \\ k_y^s \\ k_{xy}^s \end{Bmatrix}, \quad \begin{Bmatrix} \gamma_{yz} \\ \gamma_{xz} \end{Bmatrix} = g(z) \begin{Bmatrix} \gamma_{yz}^0 \\ \gamma_{xz}^0 \end{Bmatrix}, \quad \varepsilon_z = g'(z) \varepsilon_z^0 \tag{6}$$

where

$$\begin{Bmatrix} \varepsilon_x^0 \\ \varepsilon_y^0 \\ \gamma_{xy}^0 \end{Bmatrix} = \begin{Bmatrix} \frac{\partial u_0}{\partial x} \\ \frac{\partial v_0}{\partial x} \\ \frac{\partial u_0}{\partial y} + \frac{\partial v_0}{\partial x} \end{Bmatrix}, \quad \begin{Bmatrix} k_x^b \\ k_y^b \\ k_{xy}^b \end{Bmatrix} = \begin{Bmatrix} -\frac{\partial^2 w_0}{\partial x^2} \\ -\frac{\partial^2 w_0}{\partial y^2} \\ -2\frac{\partial^2 w_0}{\partial x \partial y} \end{Bmatrix}, \quad \begin{Bmatrix} k_x^s \\ k_y^s \\ k_{xy}^s \end{Bmatrix} = \begin{Bmatrix} k_1 \theta \\ k_2 \theta \\ k_1 \frac{\partial}{\partial y} \int \theta dx + k_2 \frac{\partial}{\partial x} \int \theta dy \end{Bmatrix} \quad (7a)$$

$$\begin{Bmatrix} \gamma_{yz}^0 \\ \gamma_{xz}^0 \end{Bmatrix} = \begin{Bmatrix} k_2 \int \theta dy + \frac{\partial \varphi_z}{\partial y} \\ k_1 \int \theta dx + \frac{\partial \varphi_z}{\partial x} \end{Bmatrix}, \quad \varepsilon_z^0 = \varphi_z \quad (7b)$$

The integrals used in the above equations shall be resolved by a Navier type solution and can be written as follows

$$\frac{\partial}{\partial y} \int \theta dx = A' \frac{\partial^2 \theta}{\partial x \partial y}, \quad \frac{\partial}{\partial x} \int \theta dy = B' \frac{\partial^2 \theta}{\partial x \partial y}, \quad \int \theta dx = A' \frac{\partial \theta}{\partial x}, \quad \int \theta dy = B' \frac{\partial \theta}{\partial y} \quad (8)$$

where the coefficients A' and B' are expressed according to the type of solution employed, in this case by using Navier. Therefore, A' and B' are expressed as follows

$$A' = -\frac{1}{\alpha^2}, \quad B' = -\frac{1}{\beta^2}, \quad k_1 = \alpha^2, \quad k_2 = \beta^2 \quad (9)$$

where α and β are defined in Eq. (25).

For the FG sandwich plates, the stress–strain relationships for plane-stress state including the thermal influences can be written as

$$\begin{Bmatrix} \sigma_x \\ \sigma_y \\ \sigma_z \\ \tau_{xy} \\ \tau_{xz} \\ \tau_{yz} \end{Bmatrix}^{(n)} = \begin{bmatrix} C_{11} & C_{12} & C_{13} & 0 & 0 & 0 \\ C_{12} & C_{22} & C_{23} & 0 & 0 & 0 \\ C_{13} & C_{23} & C_{33} & 0 & 0 & 0 \\ 0 & 0 & 0 & C_{66} & 0 & 0 \\ 0 & 0 & 0 & 0 & C_{55} & 0 \\ 0 & 0 & 0 & 0 & 0 & C_{44} \end{bmatrix}^{(n)} \begin{Bmatrix} \varepsilon_x - \alpha T \\ \varepsilon_y - \alpha T \\ \varepsilon_z - \alpha T \\ \gamma_{xy} \\ \gamma_{xz} \\ \gamma_{yz} \end{Bmatrix}^{(n)} \quad (10)$$

The C_{ij} expressions in terms of engineering constants are given below

$$C_{11} = C_{22} = C_{33} = \frac{E(z)}{1 - \nu^2}, \quad (11a)$$

$$C_{12} = C_{13} = C_{23} = \frac{\nu E(z)}{1 - \nu^2}, \quad (11b)$$

$$C_{44} = C_{55} = C_{66} = \frac{E(z)}{2(1 + \nu)}, \tag{11c}$$

The modulus $E(z)$ and the elastic coefficients $C_{ij}(z)$ and the thermal expansion coefficients $\alpha(z)$ change within the thickness according to Eq. (1).

The generalized temperature field which varies across the thickness of the plate can be written as follows

$$T(x, y, z) = T_1(x, y) + \frac{z}{h} T_2(x, y) + \frac{1}{\pi} \sin\left(\frac{\pi z}{h}\right) T_3(x, y) \tag{12}$$

where T_1 , T_2 and T_3 are thermal load.

2.2 Principle of virtual work (PVW)

The PVW is employed for the thermomechanical bending problem of FG sandwich plate. The PVW is expressed as

$$\delta U + \delta V = 0 \tag{13}$$

where δU is the virtual strain energy, δV is the external virtual works due to an external load applied to the plate. Substituting the appropriate energy expressions can be determined

$$\int_{-h/2}^{h/2} \int_{\Omega} [\sigma_x \delta \varepsilon_x + \sigma_y \delta \varepsilon_y + \sigma_z \delta \varepsilon_z + \tau_{xy} \delta \gamma_{xy} + \tau_{yz} \delta \gamma_{yz} + \tau_{xz} \delta \gamma_{xz}] d\Omega dz - \int_{\Omega} q \delta w d\Omega = 0 \tag{14}$$

where Ω is the top surface and q is the distributed transverse load.

Substituting Eqs. (6) and (10) into Eq. (14) and integrating within the thickness of the plate, Eq. (14) can be rewritten as

$$\int_{\Omega} [N_x \delta \varepsilon_x^0 + N_y \delta \varepsilon_y^0 + N_z \delta \varepsilon_z^0 + N_{xy} \delta \gamma_{xy}^0 + M_x^b \delta k_x^b + M_y^b \delta k_y^b + M_{xy}^b \delta k_{xy}^b + M_x^s \delta k_x^s + M_y^s \delta k_y^s + M_{xy}^s \delta k_{xy}^s + S_{yz}^s \delta \gamma_{yz}^s + S_{xz}^s \delta \gamma_{xz}^0 - q \delta w] d\Omega = 0 \tag{15}$$

where the stress resultants N , M , and S are given by

$$(N_i, M_i^b, M_i^s) = \sum_{n=1}^3 \int_{h_{n-1}}^{h_n} (1, z, f) \sigma_i^{(n)} dz, \quad (i = x, y, xy); \tag{16}$$

$$N_z = \sum_{n=1}^3 \int_{h_{n-1}}^{h_n} g'(z) \sigma_z^{(n)} dz \quad \text{and} \quad (S_{xz}^s, S_{yz}^s) = \sum_{n=1}^3 \int_{h_{n-1}}^{h_n} g(z) (\tau_{xz}, \tau_{yz})^{(n)} dz$$

where h_n and h_{n-1} are the top and bottom z -coordinates of the n th layer.

Substituting Eq. (6) into Eq. (10) and the subsequent results into Eq. (16), the stress resultants can be expressed in terms of generalized displacements $(u_0, v_0, w_0, \theta, \varphi_z)$ as

$$\begin{pmatrix} N_x \\ N_y \\ N_{xy} \\ M_x^b \\ M_y^b \\ M_{xy}^b \\ M_x^s \\ M_y^s \\ M_{xy}^s \\ N_z \end{pmatrix} = \begin{bmatrix} A_{11} & A_{12} & 0 & B_{11} & B_{12} & 0 & B_{11}^s & B_{12}^s & 0 & X_{13} \\ A_{12} & A_{22} & 0 & B_{12} & B_{22} & 0 & B_{12}^s & B_{22}^s & 0 & X_{23} \\ 0 & 0 & A_{66} & 0 & 0 & B_{66} & 0 & 0 & B_{66}^s & 0 \\ B_{11} & B_{12} & 0 & D_{11} & D_{12} & 0 & D_{11}^s & D_{12}^s & 0 & Y_{13} \\ B_{12} & B_{22} & 0 & D_{12} & D_{22} & 0 & D_{12}^s & D_{22}^s & 0 & Y_{23} \\ 0 & 0 & B_{66} & 0 & 0 & D_{66} & 0 & 0 & D_{66}^s & 0 \\ B_{11}^s & B_{12}^s & 0 & D_{11}^s & D_{12}^s & 0 & H_{11}^s & H_{12}^s & 0 & Y_{13}^s \\ B_{12}^s & B_{22}^s & 0 & D_{12}^s & D_{22}^s & 0 & H_{12}^s & H_{22}^s & 0 & Y_{23}^s \\ 0 & 0 & B_{66}^s & 0 & 0 & D_{66}^s & 0 & 0 & H_{66}^s & 0 \\ X_{13} & X_{23} & 0 & Y_{13} & Y_{23} & 0 & Y_{13}^s & Y_{23}^s & 0 & Z_{33} \end{bmatrix} \begin{pmatrix} \frac{\partial u_0}{\partial x} \\ \frac{\partial v_0}{\partial y} \\ \frac{\partial u_0}{\partial y} + \frac{\partial v_0}{\partial x} \\ -\frac{\partial^2 w_0}{\partial x^2} \\ -\frac{\partial^2 w_0}{\partial y^2} \\ -2\frac{\partial^2 w_0}{\partial x \partial y} \\ k_1 \theta \\ k_2 \theta \\ (k_1 A' + k_2 B') \frac{\partial^2 \theta}{\partial x \partial y} \\ \varphi_z \end{pmatrix} = \begin{pmatrix} N_x^T \\ N_y^T \\ 0 \\ M_x^{bT} \\ M_y^{bT} \\ 0 \\ M_x^{sT} \\ M_y^{sT} \\ 0 \\ N_z^T \end{pmatrix} \tag{17a}$$

$$\begin{pmatrix} S_{yz}^s \\ S_{xz}^s \end{pmatrix} = \begin{bmatrix} A_{44}^s & 0 \\ 0 & A_{55}^s \end{bmatrix} \begin{pmatrix} k_2 B' \frac{\partial \theta}{\partial y} + \frac{\partial \varphi_z}{\partial y} \\ k_1 A' \frac{\partial \theta}{\partial x} + \frac{\partial \varphi_z}{\partial x} \end{pmatrix} \tag{17b}$$

where

$$(A_{ij}, A_{ij}^s, B_{ij}, D_{ij}, B_{ij}^s, D_{ij}^s, H_{ij}^s) = \sum_{n=1}^3 \int_{h_{n-1}}^{h_n} C_{ij}^{(n)} (1, g^2(z), z, z^2, f(z), z f(z), f^2(z)) dz \tag{18a}$$

$$(X_{ij}, Y_{ij}, Y_{ij}^s, Z_{ij}) = \sum_{n=1}^3 \int_{h_{n-1}}^{h_n} (1, z, f(z), g'(z)) g'(z) C_{ij}^{(n)} dz \tag{18b}$$

The resultant efforts, $N_x^T = N_y^T$, $M_x^{bT} = M_y^{bT}$, $M_x^{sT} = M_y^{sT}$ and N_z^T induced by the thermal effect are expressed by

$$\begin{pmatrix} N_x^T \\ M_x^{bT} \\ M_x^{sT} \\ N_z^T \end{pmatrix} = \sum_{n=1}^3 \int_{h_{n-1}}^{h_n} \frac{E^{(n)}(z)}{1 - (\nu^{(n)})^2} (1 + 2\nu^{(n)}) \alpha^{(n)} T \begin{pmatrix} 1 \\ z \\ f(z) \\ g'(z) \end{pmatrix} dz \tag{19}$$

2.3 Plate governing equations

By employing the generalized displacement–strain expressions (Eqs. (6) and (7)) and stress–strain expressions (Eq. (10)), and integrating by parts and applying the fundamental lemma of variational calculus and collecting the coefficients of δu_0 , δv_0 , δw_0 , $\delta \theta$ and $\delta \varphi_z$ in Eq. (15), the governing equations are determined as

$$\begin{aligned}
 \delta u_0 : \quad & \frac{\partial N_x}{\partial x} + \frac{\partial N_{xy}}{\partial y} = 0 \\
 \delta v_0 : \quad & \frac{\partial N_{xy}}{\partial x} + \frac{\partial N_y}{\partial y} = 0 \\
 \delta w_0 : \quad & \frac{\partial^2 M_x^b}{\partial x^2} + 2 \frac{\partial^2 M_{xy}^b}{\partial x \partial y} + \frac{\partial^2 M_y^b}{\partial y^2} + q = 0 \\
 \delta \theta : \quad & -k_1 M_x^s - k_2 M_y^s - (k_1 A' + k_2 B') \frac{\partial^2 M_{xy}^s}{\partial x \partial y} + k_1 A' \frac{\partial S_{xz}^s}{\partial x} + k_2 B' \frac{\partial S_{yz}^s}{\partial y} = 0 \\
 \delta \varphi_z : \quad & -N_z + \frac{\partial S_{xz}^s}{\partial x} + \frac{\partial S_{yz}^s}{\partial y} = 0
 \end{aligned} \tag{20}$$

Substituting Eq. (17) into Eq. (20), the governing equations of the present quasi-3D hyperbolic shear deformation theory can be expressed in terms of displacements (u_0 , v_0 , w_0 , θ , φ_z) as

$$\begin{aligned}
 A_{11} d_{11} u_0 + A_{66} d_{22} u_0 + (A_{12} + A_{66}) d_{12} v_0 + X_{13} d_1 \varphi_z - B_{11} d_{111} w_0 - (B_{12} + 2B_{66}) d_{122} w_0 \\
 + (B_{66}^s (k_1 A' + k_2 B')) d_{122} \theta + (B_{11}^s k_1 + B_{12}^s k_2) d_1 \theta = p_1
 \end{aligned} \tag{21a}$$

$$\begin{aligned}
 A_{22} d_{22} v_0 + A_{66} d_{11} v_0 + (A_{12} + A_{66}) d_{12} u_0 + X_{23} d_2 \varphi_z - B_{22} d_{222} w_0 - (B_{12} + 2B_{66}) d_{112} w_0 \\
 + (B_{66}^s (k_1 A' + k_2 B')) d_{112} \theta + (B_{22}^s k_2 + B_{12}^s k_1) d_2 \theta = p_2
 \end{aligned} \tag{21b}$$

$$\begin{aligned}
 B_{11} d_{111} u_0 + (B_{12} + 2B_{66}) d_{122} u_0 + (B_{12} + 2B_{66}) d_{112} v_0 + B_{22} d_{222} v_0 + Y_{13} d_{11} \varphi_z + Y_{23} d_{22} \varphi_z \\
 - D_{11} d_{1111} w_0 - 2(D_{12} + 2D_{66}) d_{1122} w_0 - D_{22} d_{2222} w_0 + (D_{11}^s k_1 + D_{12}^s k_2) d_{11} \theta \\
 + 2(D_{66}^s (k_1 A' + k_2 B')) d_{1122} \theta + (D_{12}^s k_1 + D_{22}^s k_2) d_{22} \theta + q = p_3
 \end{aligned} \tag{21c}$$

$$\begin{aligned}
 - (B_{11}^s k_1 + B_{12}^s k_2) d_1 u_0 - (B_{66}^s (k_1 A' + k_2 B')) d_{122} u_0 - (B_{66}^s (k_1 A' + k_2 B')) d_{112} v_0 \\
 - (B_{12}^s k_1 + B_{22}^s k_2) d_2 v_0 - k_1 Y_{13}^s \varphi_z - k_2 Y_{23}^s \varphi_z + (D_{11}^s k_1 + D_{12}^s k_2) d_{11} w_0 + 2(D_{66}^s (k_1 A' + k_2 B')) d_{1122} w_0 \\
 + (D_{12}^s k_1 + D_{22}^s k_2) d_{22} w_0 - H_{11}^s k_1^2 \theta - H_{22}^s k_2^2 \theta - 2H_{12}^s k_1 k_2 \theta - ((k_1 A' + k_2 B')^2 H_{66}^s) d_{1122} \theta \\
 + A_{44}^s (k_2 B')^2 d_{22} \theta + A_{55}^s (k_1 A')^2 d_{11} \theta + A_{44}^s (k_2 B') d_{22} \varphi_z + A_{55}^s (k_1 A') d_{11} \varphi_z = p_4
 \end{aligned} \tag{21d}$$

$$\begin{aligned}
 - X_{13} d_1 u_0 - X_{23} d_2 v_0 - Z_{33} \varphi_z + Y_{13} d_{11} w_0 + Y_{23} d_{22} w_0 \\
 + (A_{44}^s - Y_{23}^s) (k_2 B') d_{22} \theta + (A_{55}^s - Y_{13}^s) (k_1 A') d_{11} \theta + A_{44}^s d_{22} \varphi_z + A_{55}^s d_{11} \varphi_z = p_5
 \end{aligned} \tag{21e}$$

where d_{ij} , d_{ijl} and d_{ijlm} are the following differential operators

$$d_{ij} = \frac{\partial^2}{\partial x_i \partial x_j}, \quad d_{ijl} = \frac{\partial^3}{\partial x_i \partial x_j \partial x_l}, \quad d_{ijlm} = \frac{\partial^4}{\partial x_i \partial x_j \partial x_l \partial x_m}, \quad d_i = \frac{\partial}{\partial x_i}, \quad (i, j, l, m = 1, 2). \quad (22)$$

The components of the generalized force vector $\{p\}$ are given by

$$p_1 = \frac{\partial N_x^T}{\partial x}, \quad p_2 = \frac{\partial N_y^T}{\partial y}, \quad p_3 = q - \frac{\partial^2 M_x^{bT}}{\partial x^2} - \frac{\partial^2 M_y^{bT}}{\partial y^2}, \quad p_4 = q - \frac{\partial^2 M_x^{sT}}{\partial x^2} - \frac{\partial^2 M_y^{sT}}{\partial y^2}, \quad p_5 = N_z^T \quad (23)$$

3. Solution procedure

Consider a simply supported rectangular plate with length a and width b under transverse load q . To solve this problem, Navier presented the transverse mechanical and temperature loads q , T_1 , T_2 , and T_3 in the form of a double trigonometric series as

$$\begin{Bmatrix} q \\ T_1 \\ T_2 \\ T_3 \end{Bmatrix} = \begin{Bmatrix} q_0 \\ t_1 \\ t_2 \\ t_3 \end{Bmatrix} \sin(\alpha x) \sin(\beta y) \quad (24)$$

where q_0 , t_1 , t_2 , and t_3 are constants, α and β are given by

$$\alpha = m\pi/a \quad \text{and} \quad \beta = n\pi/b \quad (25)$$

By employing Navier's procedure, the solution of the displacement variables satisfying the above boundary conditions can be written in the following Fourier series

$$\begin{Bmatrix} u_0 \\ v_0 \\ w_0 \\ \theta \\ \varphi_z \end{Bmatrix} = \begin{Bmatrix} U \cos(\alpha x) \sin(\beta y) \\ V \sin(\alpha x) \cos(\beta y) \\ W \sin(\alpha x) \sin(\beta y) \\ X \sin(\alpha x) \sin(\beta y) \\ \Phi \sin(\alpha x) \sin(\beta y) \end{Bmatrix} \quad (26)$$

where (U, V, W, X, Φ) are unknown functions to be determined. By considering Eqs. (18) and (23), the following equation is obtained

$$\begin{bmatrix} S_{11} & S_{12} & S_{13} & S_{14} & S_{15} \\ S_{12} & S_{22} & S_{23} & S_{24} & S_{25} \\ S_{13} & S_{23} & S_{33} & S_{34} & S_{35} \\ S_{14} & S_{24} & S_{34} & S_{44} & S_{45} \\ S_{15} & S_{25} & S_{35} & S_{45} & S_{55} \end{bmatrix} \begin{Bmatrix} U \\ V \\ W \\ X \\ \Phi \end{Bmatrix} = \begin{Bmatrix} P_1 \\ P_2 \\ P_3 \\ P_4 \\ P_5 \end{Bmatrix} \quad (27)$$

where

$$\begin{aligned}
 S_{11} &= \alpha^2 B_{11} + \beta^2 A_{66}, & S_{12} &= \alpha\beta(A_{12} + A_{66}), & S_{13} &= -\alpha^3 B_{11} - \alpha\beta^2(B_{12} + 2B_{66}) \\
 S_{14} &= -\alpha(k_1 B_{11}^s + k_2 B_{12}^s) + \alpha\beta^2 B_{66}^s(k_1 A' + k_2 B'), & S_{15} &= \alpha X_{13} \\
 S_{22} &= \alpha^2 A_{66} + \beta^2 A_{22}, & S_{23} &= -\alpha^2\beta(B_{12} + 2B_{66}) - \beta^3 B_{22} \\
 S_{24} &= -\beta(k_1 B_{12}^s + k_2 B_{22}^s) + \alpha^2\beta(k_1 A' + k_2 B')B_{66}^s, & S_{25} &= -\beta X_{23} \\
 S_{33} &= \alpha^4 D_{11} + \beta^4 D_{22} + 2\alpha^2\beta^2(D_{12} + 2D_{66}) \\
 S_{34} &= \alpha^2 k_1 D_{11}^s + (k_2\alpha^2 + k_1\beta^2)D_{12}^s + \beta^2 k_2 D_{22}^s - 2\alpha^2\beta^2(k_1 A' + k_2 B')D_{66}^s, & S_{35} &= \alpha^2 Y_{13} + \beta^2 Y_{23} \\
 S_{44} &= k_1^2 H_{11}^s + k_2^2 H_{22}^s + 2k_1 k_2 H_{12}^s + \alpha^2\beta^2(k_1 A' + k_2 B')^2 H_{66}^s + \alpha^2(k_1 A')^2 A_{55}^s + \beta^2(k_2 B')^2 A_{44}^s \\
 S_{45} &= k_1 Y_{13}^s + k_2 Y_{23}^s + \alpha^2 k_1 A' A_{55}^s + \beta^2 k_2 B' A_{44}^s, & S_{55} &= \alpha^2 A_{55}^s + \beta^2 A_{44}^s + Z_{33}
 \end{aligned} \tag{28}$$

and the components of the generalized force vector $\{P\} = \{P_1, P_2, P_3, P_4, P_5\}^t$ are expressed by

$$\begin{aligned}
 P_1 &= \lambda(A^T t_1 + B^T t_2 + {}^a B^T t_3), \\
 P_2 &= \mu(A^T t_1 + B^T t_2 + {}^a B^T t_3), \\
 P_3 &= -q_0 - h(\lambda^2 + \mu^2)(B^T t_1 + D^T t_2 + {}^a D^T t_3), \\
 P_4 &= -q_0 - h(\lambda^2 + \mu^2)({}^s B^T t_1 + {}^s D^T t_2 + {}^s F^T t_3), \\
 P_5 &= -h(L^T t_1 + {}^a L^T t_2 + R^T t_3).
 \end{aligned} \tag{29}$$

where

$$(A^T, B^T, D^T) = \sum_{n=1}^3 \int_{h_{n-1}}^{h_n} \frac{E^{(n)}(z)}{1 - (\nu^{(n)})^2} (1 + 2\nu^{(n)}) \alpha^{(n)}(1, \bar{z}, \bar{z}^2) dz, \tag{30a}$$

$$({}^a B^T, {}^a D^T) = \sum_{n=1}^3 \int_{h_{n-1}}^{h_n} \frac{E^{(n)}(z)}{1 - (\nu^{(n)})^2} (1 + 2\nu^{(n)}) \alpha^{(n)} \bar{\Psi}(z)(1, \bar{z}) dz, \tag{30b}$$

$$({}^s B^T, {}^s D^T, {}^s F^T) = \sum_{n=1}^3 \int_{h_{n-1}}^{h_n} \frac{E^{(n)}(z)}{1 - (\nu^{(n)})^2} (1 + 2\nu^{(n)}) \alpha^{(n)} \bar{f}(z)(1, \bar{z}, \bar{\Psi}(z)) dz, \tag{30c}$$

$$(L^T, L_a^T, R^T) = \sum_{n=1}^3 \int_{h_{n-1}}^{h_n} \frac{E^{(n)}(z)}{1 - (\nu^{(n)})^2} (1 + 2\nu^{(n)}) \alpha^{(n)} \bar{g}'(z)(1, \bar{z}, \bar{\Psi}(z)) dz, \tag{30d}$$

with $\bar{z} = z/h, \bar{f}(z) = f(z)/h$ and $\bar{\Psi}(z) = \frac{1}{\pi} \sin\left(\frac{\pi z}{h}\right)$.

4. Numerical results and discussion

In this section the results of the thermomechanical bending analysis of FG sandwich plates are presented. The present results are computed using the present new quasi-3D type HSDT with only 5 unknowns. The theory is formulated in such way that the thickness stretching influence is considered, i.e. the Koiter’s recommendation regarding stretching influence of the plate (Koiter 1959) is obeyed. Typical mechanical properties for metal and ceramics employed in the numerical examples are listed in Table 1.

The results are presented in the following normalized forms for displacements and stresses according to Saidi *et al.* (2013) for the purpose of presentation in this article.

- Center deflection $\bar{w} = \frac{10^3}{q_0 a^4 / (E_0 h^3) + 10^3 \alpha_0 t_2 a^2 / h} w\left(\frac{a}{2}, \frac{b}{2}\right)$,
- Axial stress $\bar{\sigma}_x = \frac{10}{q_0 a^2 / h^2 + 10 E_0 \alpha_0 t_2 a^2 / h^2} \sigma_x\left(\frac{a}{2}, \frac{b}{2}, \frac{h}{2}\right)$,
- Shear stress $\bar{\tau}_{xz} = \frac{1}{q_0 a / h + E_0 \alpha_0 t_2 a / 10 h} \tau_{xz}\left(0, \frac{b}{2}, 0\right)$,

where the reference values are taken as $E_0 = 1$ GPa and $\alpha_0 = 10^{-6} / K$.

It is assumed, unless otherwise stated, that $a / h = 10$, $a / b = 1$, $t_1 = 0$, and $q_0 = t_2 = t_3 = 100$. The shear correction factor of FSDT is fixed to be $K = 5 / 6$.

Examination of Tables 2-5 reveals that the present theory with only five variables provides similar results to those computed by the hyperbolic plate theory (HPT) proposed by Saidi *et al.* (2013) and the sinusoidal plate theory (SPT) developed by Zenkour and Alghamdi (2008) with six unknowns ($\varepsilon_z \neq 0$). This demonstrates that the same accuracy is achievable with the present theory using a lower number of variables than other theories, and clearly highlights how the present model is simpler and more easily deployed.

Table 2 presents results of non-dimensional deflections \bar{w} of FG sandwich plates for various sandwich schemes and exponents “ k ”. The sandwich plate is subjected to a linear temperature distribution through the thickness. The present results are compared with solutions based on a refined HPT (Saidi *et al.* 2013) and SPT proposed by Zenkour and Alghamdi (2008). From this table it can be seen that the present results are lower than the solution given by Zenkour and Alghamdi (2008) without considering the thickness stretching ($\varepsilon_z = 0$). Hence, Table 2 demonstrates that the influence of the thickness stretching is to reduce the deflection. The non-dimensional deflection increases as the exponent “ k ” increases. However, this effect decreases for higher values of the exponent “ k ”.

Table 1 Material properties of the used FG sandwich plates

Material	Properties		
	E (GPa)	α ($10^{-6}/K$)	ν
Metal: Ti-6Al-4V	66.2	10.3	1/3
Ceramic: ZrO ₂	117.0	7.11	1/3

Table 3 Continued

k	Theory	\bar{w}					
		$t_{FGM}/h = 0$	$t_{FGM}/h = 0.2$	$t_{FGM}/h = 0.4$	$t_{FGM}/h = 0.6$	$t_{FGM}/h = 0.8$	$t_{FGM}/h = 1$
1	Present ($\varepsilon_z \neq 0$)	0,750266	0,835477	0,909406	0,965390	1,001361	1,022245
	Ref ^(a) ($\varepsilon_z \neq 0$)	0,748424	0,825607	0,891560	0,942936	0,979382	1,003408
	SSDT ($\varepsilon_z = 0$)	0,796783	0,873745	0,941636	0,996334	1,036213	1,062840
	TSDT ($\varepsilon_z = 0$)	0,806067	0,886067	0,954808	1,010231	1,050672	1,077690
	FSDT ($\varepsilon_z = 0$)	0,895735	0,979641	1,054630	1,115684	1,160568	1,190728
	CPT ($\varepsilon_z = 0$)	0,457873	0,501163	0,539886	0,571450	0,594688	0,610331
	2	Present ($\varepsilon_z \neq 0$)	0,750266	0,857801	0,953182	1,022704	1,060581
Ref ^(a) ($\varepsilon_z \neq 0$)		0,748424	0,845883	0,930539	0,994421	1,035346	1,057609
SSDT ($\varepsilon_z = 0$)		0,796783	0,894003	0,981434	1,050237	1,096095	1,121608
TSDT ($\varepsilon_z = 0$)		0,806067	0,906529	0,995042	1,064791	1,111352	1,137297
FSDT ($\varepsilon_z = 0$)		0,895735	1,001204	1,097973	1,175402	1,227765	1,257304
CPT ($\varepsilon_z = 0$)		0,457873	0,512431	0,562536	0,602673	0,629859	0,645223
3		Present ($\varepsilon_z \neq 0$)	0,750266	0,868264	0,973510	1,047444	1,082097
	Ref ^(a) ($\varepsilon_z \neq 0$)	0,748424	0,855272	0,948423	1,016599	1,056867	1,075460
	SSDT ($\varepsilon_z = 0$)	0,796783	0,903467	0,999831	1,073875	1,119794	1,141655
	TSDT ($\varepsilon_z = 0$)	0,806067	0,916083	1,013647	1,088747	1,135420	1,157693
	FSDT ($\varepsilon_z = 0$)	0,895735	1,011279	1,118224	1,202080	1,255041	1,280741
	CPT ($\varepsilon_z = 0$)	0,457873	0,517716	0,573152	0,616662	0,644176	0,657539
	4	Present ($\varepsilon_z \neq 0$)	0,750266	0,874328	0,985072	1,060516	1,091512
Ref ^(a) ($\varepsilon_z \neq 0$)		0,748424	0,902511	0,958901	1,028393	1,067181	1,082846
SSDT ($\varepsilon_z = 0$)		0,796783	0,908934	1,010269	1,086624	1,131429	1,150192
TSDT ($\varepsilon_z = 0$)		0,806067	0,921602	1,024208	1,101684	1,147260	1,166403
FSDT ($\varepsilon_z = 0$)		0,895735	1,017115	1,129824	1,216678	1,268689	1,290961
CPT ($\varepsilon_z = 0$)		0,457873	0,520783	0,579240	0,624324	0,651345	0,662909
5		Present ($\varepsilon_z \neq 0$)	0,750266	0,878280	0,992466	1,068336	1,096132
	Ref ^(a) ($\varepsilon_z \neq 0$)	0,748424	0,864347	0,943749	1,034550	1,072864	1,086419
	SSDT ($\varepsilon_z = 0$)	0,796783	0,912488	1,016938	1,094427	1,137993	1,154412
	TSDT ($\varepsilon_z = 0$)	0,806067	0,925190	1,030958	1,109609	1,153952	1,170720
	FSDT ($\varepsilon_z = 0$)	0,895735	1,020919	1,137289	1,225706	1,276497	1,296101
	CPT ($\varepsilon_z = 0$)	0,457873	0,522783	0,583160	0,629064	0,655445	0,665606

^(a) Taken from Hamidi *et al.* (2015)

Table 3 compares the deflections of different types of FG square sandwich plates for $k=0, 1, 2, 3, 4,$ and 5 . The present results are compared with solutions based on a sinusoidal shear deformation theory (SSDT), third shear deformation theory (TSDT), first shear deformation theory (FSDT) and classical plate theory (CPT). It can be concluded that the introduction of thickness stretching influence serves to make the plate stiffer, and hence, leads to a reduction of deflection.

However, the introduction of shear deformation influence makes the plate more flexible and consequently leads to increase the deflection.

Table 4 presents results of non-dimensional deflections “ \bar{w} ” of FG sandwich plates for different values of aspect ratio “ a / b ” and several sandwich schemes, considering an exponent $k = 3$. The results are compared with HSDTs, FSDT and CPT as in Table 3. It can be seen that the deflection increases with the increasing thickness of the FG layer (t_{FGM}) and it is reduced with increasing the aspect ratio a / b .

Table 4 Effect of aspect ratio a / b on the dimensionless deflection \bar{w} of the FG sandwich plates ($k = 3$)

t_{FGM} / h	Theory	$a / b = 1$	$a / b = 2$	$a / b = 3$	$a / b = 4$	$a / b = 5$
0	Present ($\varepsilon_z \neq 0$)	0,750266	0,278996	0,102301	0,043917	0,021319
	HSDT ($\varepsilon_z = 0$)	0,817556	0,321791	0,159940	0,093790	0,061185
	SSDT ($\varepsilon_z = 0$)	0,796783	0,313432	0,155719	0,091273	0,059512
	TSDT ($\varepsilon_z = 0$)	0,808168	0,318014	0,158033	0,092654	0,060430
	FSDT ($\varepsilon_z = 0$)	0,895735	0,353189	0,175744	0,103172	0,067392
	CPT ($\varepsilon_z = 0$)	0,457873	0,178044	0,088171	0,051659	0,033711
0,2	Present ($\varepsilon_z \neq 0$)	0,868264	0,316806	0,116340	0,049971	0,024264
	HSDT ($\varepsilon_z = 0$)	0,926476	0,364706	0,181529	0,106696	0,069818
	SSDT ($\varepsilon_z = 0$)	0,903467	0,355510	0,176937	0,104000	0,068059
	TSDT ($\varepsilon_z = 0$)	0,916083	0,360554	0,179457	0,105480	0,069026
	FSDT ($\varepsilon_z = 0$)	1,011279	0,398391	0,198176	0,116327	0,075980
	CPT ($\varepsilon_z = 0$)	0,517716	0,200966	0,099463	0,058261	0,038014
0,4	Present ($\varepsilon_z \neq 0$)	0,973510	0,351873	0,129328	0,055567	0,026986
	HSDT ($\varepsilon_z = 0$)	1,025027	0,403196	0,200642	0,117924	0,077167
	SSDT ($\varepsilon_z = 0$)	0,999831	0,393146	0,195642	0,115002	0,075273
	TSDT ($\varepsilon_z = 0$)	1,013647	0,398658	0,198386	0,116606	0,076314
	FSDT ($\varepsilon_z = 0$)	1,118224	0,440203	0,218920	0,128491	0,083921
	CPT ($\varepsilon_z = 0$)	0,573152	0,222174	0,109906	0,064364	0,041992
0,6	Present ($\varepsilon_z \neq 0$)	1,047444	0,378793	0,139244	0,059831	0,029058
	HSDT ($\varepsilon_z = 0$)	1,101003	0,432682	0,215157	0,126351	0,082600
	SSDT ($\varepsilon_z = 0$)	1,073875	0,421843	0,209748	0,123178	0,080532
	TSDT ($\varepsilon_z = 0$)	1,088747	0,427786	0,212715	0,124919	0,081668
	FSDT ($\varepsilon_z = 0$)	1,202080	0,472957	0,235166	0,138015	0,090138
	CPT ($\varepsilon_z = 0$)	1,202080	0,238790	0,118083	0,069142	0,045106
0,8	Present ($\varepsilon_z \neq 0$)	1,082097	0,394673	0,145028	0,062309	0,030259
	HSDT ($\varepsilon_z = 0$)	1,148302	0,450940	0,224088	0,131493	0,085879
	SSDT ($\varepsilon_z = 0$)	1,119794	0,439521	0,218366	0,128116	0,083662
	TSDT ($\varepsilon_z = 0$)	1,135420	0,445781	0,221504	0,129968	0,084879
	FSDT ($\varepsilon_z = 0$)	1,255041	0,493613	0,245406	0,144017	0,094055
	CPT ($\varepsilon_z = 0$)	0,644176	0,249267	0,123233	0,072151	0,047066

Table 4 Continued

t_{FGM} / h	Theory	$a / b = 1$	$a / b = 2$	$a / b = 3$	$a / b = 4$	$a / b = 5$
1	Present ($\varepsilon_z \neq 0$)	1,090461	0,354791	0,147526	0,063373	0,030774
	HSDT ($\varepsilon_z = 0$)	1,170917	0,459613	0,228305	0,133902	0,087401
	SSDT ($\varepsilon_z = 0$)	1,141655	0,447872	0,222403	0,130406	0,085094
	TSDT ($\varepsilon_z = 0$)	1,157693	0,454308	0,225639	0,132324	0,086360
	FSDT ($\varepsilon_z = 0$)	1,280741	0,503607	0,250355	0,146917	0,095948
	CPT ($\varepsilon_z = 0$)	0,657539	0,254326	0,125715	0,073599	0,048009

Tables 5 and 6 present, respectively, the axial stress “ $\bar{\sigma}_x$ ” and transverse shear stress “ $\bar{\tau}_{xz}$ ” for $k = 0, 1, 2, 3, 4$ and 5 and different FG layer thickness (t_{FGM}). It can be seen that the axial stress $\bar{\sigma}_x$ and transverse shear stress $\bar{\tau}_{xz}$ are very sensitive to the variation of the exponent “ k ” and FG layer thickness. As is demonstrated in the case of deflections, the thickness stretching influence leads also to a reduction of stresses. It can be concluded from Tables 3-6 that the introduction of thickness stretching influence makes a plate stiffer, and hence, leads to a reduction of deflection and stresses.

Table 5 Dimensionless axial stresses $\bar{\sigma}_x$ of different sandwich squares plates

k	Theory	$\bar{\sigma}_x$					
		$t_{FGM} / h = 0$	$t_{FGM} / h = 0.2$	$t_{FGM} / h = 0.4$	$t_{FGM} / h = 0.6$	$t_{FGM} / h = 0.8$	$t_{FGM} / h = 1$
0	Present ($\varepsilon_z \neq 0$)	-1,948246	-1,948246	-1,948246	-1,948246	-1,948246	-1,948246
	Ref ^(a) ($\varepsilon_z \neq 0$)	-1,650736	-1,650736	-1,650736	-1,650736	-1,650736	-1,650736
	Ref ^(b) ($\varepsilon_z \neq 0$)	-2,528819	-2,528819	-2,528819	-2,528819	-2,528819	-2,528819
	SSDT ($\varepsilon_z = 0$)	-2,388919	-2,388919	-2,388919	-2,388919	-2,388919	-2,388919
	TSDT ($\varepsilon_z = 0$)	-2,461177	-2,461177	-2,461177	-2,461177	-2,461177	-2,461177
	FSDT ($\varepsilon_z = 0$)	-3,597007	-3,597007	-3,597007	-3,597007	-3,597007	-3,597007
	CPT ($\varepsilon_z = 0$)	-1,706393	-1,706393	-1,706393	-1,706393	-1,706393	-1,706393
1	Present ($\varepsilon_z \neq 0$)	-1,948246	-3,610619	-3,146952	-2,781299	-2,518922	-2,345486
	Ref ^(a) ($\varepsilon_z \neq 0$)	-1,650736	-3,372080	-2,859305	-2,461461	-2,179138	-1,993540
	Ref ^(b) ($\varepsilon_z \neq 0$)	-2,528819	-3,913321	-3,245326	-3,245326	-2,797887	-2,316178
	SSDT ($\varepsilon_z = 0$)	-2,388919	-3,333300	-3,001265	-2,733086	-2,537374	-2,406806
	TSDT ($\varepsilon_z = 0$)	-2,461177	-3,412724	-3,076466	-2,804750	-2,606343	-2,473909
	FSDT ($\varepsilon_z = 0$)	-3,597007	-4,504051	-4,136892	-3,838047	-3,618476	-3,411099
	CPT ($\varepsilon_z = 0$)	-1,706393	-3,610619	-3,146952	-2,781299	-2,518922	-2,345486
2	Present ($\varepsilon_z \neq 0$)	-1,948246	-3,469271	-2,874730	-2,419587	-2,122935	-1,960660
	Ref ^(a) ($\varepsilon_z \neq 0$)	-1,650736	-3,211762	-2,556774	-2,066031	-1,751165	-1,580468
	Ref ^(b) ($\varepsilon_z \neq 0$)	-2,528819	-3,792865	-3,245326	-2,645068	-2,332424	-2,180056
	SSDT ($\varepsilon_z = 0$)	-2,388919	-3,234499	-2,806645	-2,469045	-2,243809	-2,118730
	TSDT ($\varepsilon_z = 0$)	-2,461177	-3,312889	-2,879670	-2,537489	-2,308903	-2,181780
	FSDT ($\varepsilon_z = 0$)	-3,597007	-4,398484	-3,924721	-3,545789	-3,289757	-3,145662
	CPT ($\varepsilon_z = 0$)	-1,706393	-3,469271	-2,874730	-2,419587	-2,122935	-1,960660

Table 5 Continued

k	Theory	$\bar{\sigma}_x$					
		$t_{FGM}/h = 0$	$t_{FGM}/h = 0.2$	$t_{FGM}/h = 0.4$	$t_{FGM}/h = 0.6$	$t_{FGM}/h = 0.8$	$t_{FGM}/h = 1$
3	Present ($\varepsilon_z \neq 0$)	-1,948246	-3,403457	-2,750142	-2,263590	-1,969619	-1,832782
	Ref ^(a) ($\varepsilon_z \neq 0$)	-1,650736	-3,137344	-2,419727	-1,898185	-1,588667	-1,446122
	Ref ^(b) ($\varepsilon_z \neq 0$)	-2,528819	-3,736478	-3,130873	-1,898185	-1,588667	-1,446122
	SSDT ($\varepsilon_z = 0$)	-2,388919	-3,188312	-2,716593	-2,353122	-2,127496	-2,020425
	TSDT ($\varepsilon_z = 0$)	-2,461177	-3,266245	-2,788595	-2,420027	-2,190823	-2,081815
	FSDT ($\varepsilon_z = 0$)	-3,597007	-4,349165	-3,825600	-3,415261	-3,156414	-3,031283
4	Present ($\varepsilon_z \neq 0$)	-1,948246	-3,365540	-2,679970	-2,180433	-1,895490	-1,779386
	Ref ^(a) ($\varepsilon_z \neq 0$)	-1,650736	-3,094600	-2,343139	-1,809688	-1,511078	-1,390767
	Ref ^(b) ($\varepsilon_z \neq 0$)	-2,528819	-3,703803	-3,065266	-2,561174	-2,252973	-2,120478
	SSDT ($\varepsilon_z = 0$)	-2,388919	-3,161620	-2,665468	-2,290552	-2,070361	-1,978602
	TSDT ($\varepsilon_z = 0$)	-2,461177	-3,239292	-2,736867	-2,356554	-2,132710	-2,039172
	FSDT ($\varepsilon_z = 0$)	-3,597007	-4,320597	-3,768831	-3,343853	-3,089733	-2,981507
5	Present ($\varepsilon_z \neq 0$)	-1,948246	-3,340946	-2,6353801	-2,129968	-1,655927	-1,603084
	Ref ^(a) ($\varepsilon_z \neq 0$)	-1,650736	-3,066950	-2,294758	-1,756372	-1,468147	-1,446122
	Ref ^(b) ($\varepsilon_z \neq 0$)	-2,528819	-3,682505	-3,023018	-2,509154	-2,207341	-2,2090458
	SSDT ($\varepsilon_z = 0$)	-2,388919	-3,682505	-2,632792	-2,252244	-2,038118	-1,957968
	TSDT ($\varepsilon_z = 0$)	-2,461177	-3,221769	-2,703791	-2,317655	-2,099863	-2,018086
	FSDT ($\varepsilon_z = 0$)	-3,597007	-4,301976	-3,732298	-3,299697	-3,051612	-2,956534

^(a) Taken from Saidi *et al.* (2013)

^(b) Taken from Hamidi *et al.* (2015)

Table 6 Dimensionless transverse shear stresses $\bar{\tau}_{xz}$ of different sandwich squares plates

k	Theory	$\bar{\tau}_{xz}$					
		$t_{FGM}/h = 0$	$t_{FGM}/h = 0.2$	$t_{FGM}/h = 0.4$	$t_{FGM}/h = 0.6$	$t_{FGM}/h = 0.8$	$t_{FGM}/h = 1$
0	Present ($\varepsilon_z \neq 0$)	0,152386	0,152386	0,152386	0,152386	0,152386	0,152386
	Ref ^(a) ($\varepsilon_z \neq 0$)	0,142427	0,142427	0,142427	0,142427	0,142427	0,142427
	Ref ^(b) ($\varepsilon_z \neq 0$)	0,194197	0,194197	0,194197	0,194197	0,194197	0,194197
	SSDT ($\varepsilon_z = 0$)	0,171604	0,171604	0,171604	0,171604	0,171604	0,171604
	TSDT ($\varepsilon_z = 0$)	0,174481	0,174481	0,174481	0,174481	0,174481	0,174481
	FSDT ($\varepsilon_z = 0$)	0,173624	0,173624	0,173624	0,173624	0,173624	0,173624
1	Present ($\varepsilon_z \neq 0$)	0,152386	0,236112	0,231170	0,235860	0,248341	0,267823
	Ref ^(a) ($\varepsilon_z \neq 0$)	0,142427	0,245892	0,271139	0,263095	0,250022	0,245207
	Ref ^(b) ($\varepsilon_z \neq 0$)	0,194197	0,358090	0,346354	0,370811	0,315647	0,308622
	SSDT ($\varepsilon_z = 0$)	0,171604	0,271618	0,300335	0,293865	0,280890	0,277019
	TSDT ($\varepsilon_z = 0$)	0,174481	0,264677	0,285938	0,284236	0,274133	0,272347
	FSDT ($\varepsilon_z = 0$)	0,173624	0,181504	0,190134	0,199626	0,210115	0,221768

Table 6 Continued

k	Theory	\bar{w}_{xz}					
		$t_{FGM} / h = 0$	$t_{FGM} / h = 0.2$	$t_{FGM} / h = 0.4$	$t_{FGM} / h = 0.6$	$t_{FGM} / h = 0.8$	$t_{FGM} / h = 1$
2	Present ($\varepsilon_z \neq 0$)	0,152386	0,232742	0,228551	0,238272	0,260030	0,294507
	Ref ^(a) ($\varepsilon_z \neq 0$)	0,142427	0,266548	0,287189	0,265885	0,243455	0,239333
	Ref ^(b) ($\varepsilon_z \neq 0$)	0,194197	0,368104	0,341227	0,376236	0,315647	0,308622
	SSDT ($\varepsilon_z = 0$)	0,171604	0,292205	0,317892	0,298078	0,275130	0,272583
	TSDT ($\varepsilon_z = 0$)	0,174481	0,282950	0,304910	0,288355	0,270427	0,270952
	FSDT ($\varepsilon_z = 0$)	0,173624	0,185719	0,199626	0,215785	0,225945	0,244354
3	Present ($\varepsilon_z \neq 0$)	0,152386	0,231344	0,228089	0,241321	0,269479	0,315305
	Ref ^(a) ($\varepsilon_z \neq 0$)	0,142427	0,274786	0,291316	0,261357	0,235362	0,235593
	Ref ^(b) ($\varepsilon_z \neq 0$)	0,194197	0,348104	0,376236	0,341227	0,304511	0,302325
	SSDT ($\varepsilon_z = 0$)	0,171604	0,300600	0,322239	0,294047	0,267073	0,269608
	TSDT ($\varepsilon_z = 0$)	0,174481	0,290349	0,308697	0,285154	0,264327	0,270110
	FSDT ($\varepsilon_z = 0$)	0,173624	0,185719	0,199626	0,215785	0,234789	0,257465
4	Present ($\varepsilon_z \neq 0$)	0,152386	0,230598	0,228124	0,243864	0,276659	0,331357
	Ref ^(a) ($\varepsilon_z \neq 0$)	0,142427	0,279028	0,291316	0,257131	0,230171	0,235324
	Ref ^(b) ($\varepsilon_z \neq 0$)	0,194197	0,373398	0,336004	0,377769	0,296906	0,300779
	SSDT ($\varepsilon_z = 0$)	0,171604	0,305016	0,323396	0,289951	0,261729	0,270017
	TSDT ($\varepsilon_z = 0$)	0,174481	0,294226	0,309711	0,281837	0,260366	0,271755
	FSDT ($\varepsilon_z = 0$)	0,173624	0,186586	0,201639	0,219335	0,240436	0,266029
5	Present ($\varepsilon_z \neq 0$)	0,152386	0,230141	0,228291	0,245894	0,282200	0,344022
	Ref ^(a) ($\varepsilon_z \neq 0$)	0,142427	0,281670	0,291163	0,253889	0,227025	0,236707
	Ref ^(b) ($\varepsilon_z \neq 0$)	0,194197	0,377010	0,331797	0,378075	0,292003	0,319732
	SSDT ($\varepsilon_z = 0$)	0,171604	0,307694	0,323573	0,286687	0,258433	0,272071
	TSDT ($\varepsilon_z = 0$)	0,174481	0,296571	0,309879	0,279200	0,258029	0,274512
	FSDT ($\varepsilon_z = 0$)	0,173624	0,187168	0,203004	0,221768	0,244354	0,272062

^(a) Taken from Saidi *et al.* (2013)

^(b) Taken from Hamidi *et al.* (2015)

Fig. 2 demonstrates the influence of the aspect ratio a / b on the non-dimensional center deflection \bar{w} for FG sandwich plate. The influences of the mechanical and thermal loads are considered in this example. From Fig. 2, it can be noticed that the aspect ratio influence is more pronounced on the thermomechanical bending deflection \bar{w} ($q_0 = t_2 = t_3 = 100$) of the FG sandwich plate.

Fig. 3 shows the variation of the non-dimensional deflection \bar{w} as a function of the aspect ratio a / b of the metal plate, ceramic plate and FG sandwich plate ($k = 1.5$). It is found that the deflection is maximum for the metallic plate and minimum for the ceramic plate.

Fig. 4 shows the effect of the side-to-thickness ratio a / h on the non-dimensional center deflection \bar{w} for FG sandwich plate. The influences of the mechanical and thermal loads are

taken into account in this example. In Fig. 4 it can be seen that the thermomechanical loading ($q_0 = t_2 = t_3 = 100$) significantly influences the results of the non-dimensional deflection.

Fig. 5 presents the variation of the center deflection \bar{w} with side-to-thickness ratio a/h for FG sandwich plates. The deflection of the metallic plate is found to be the largest magnitude and that of the ceramic plate of the smallest magnitude. It is to be noted that the FG sandwich plates with intermediate properties undergo corresponding intermediate values of center deflection. This is expected because the metallic plate is the one with the lowest stiffness and the ceramic plate is the one with the highest stiffness.

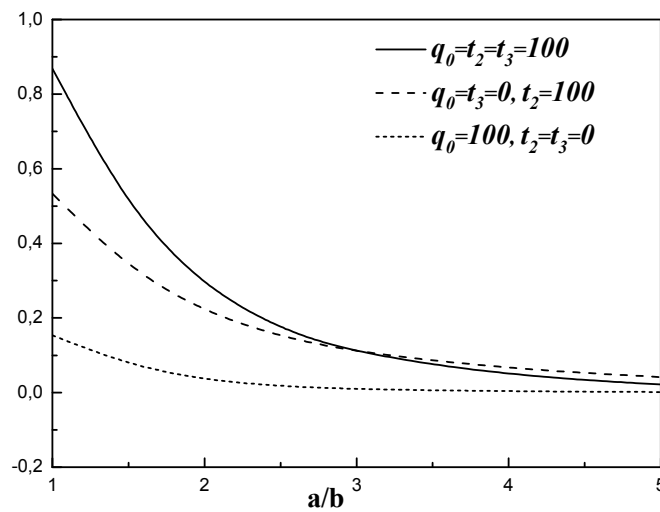


Fig. 2 Influence of mechanical and thermal loads on the dimensionless center deflection of FG sandwich plate versus a/b ($t_{FGM} = 0.2h, k = 3$)

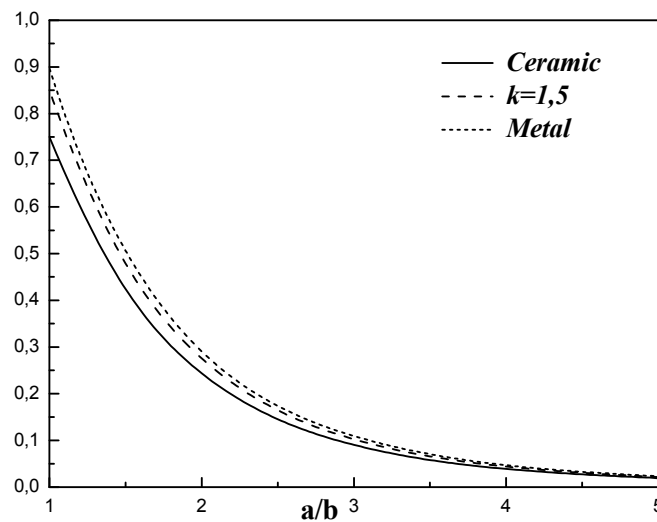


Fig. 3 Effect of the aspect ratio a/b on dimensionless center deflection for FG sandwich plates ($t_{FGM} = 0.2h, t_1 = 10, q_0 = t_2 = t_3 = 100$)

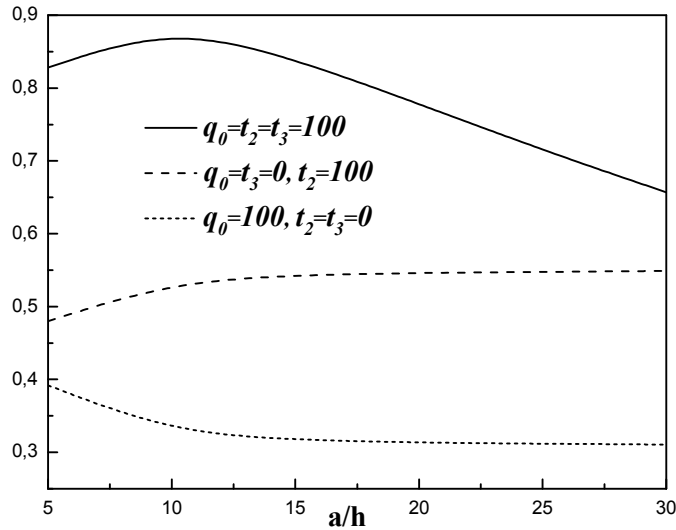


Fig. 4 Effect of mechanical and thermal loads on the dimensionless center deflection of FG sandwich plate versus a/h ($t_{FGM} = 0.2h, k = 3$)

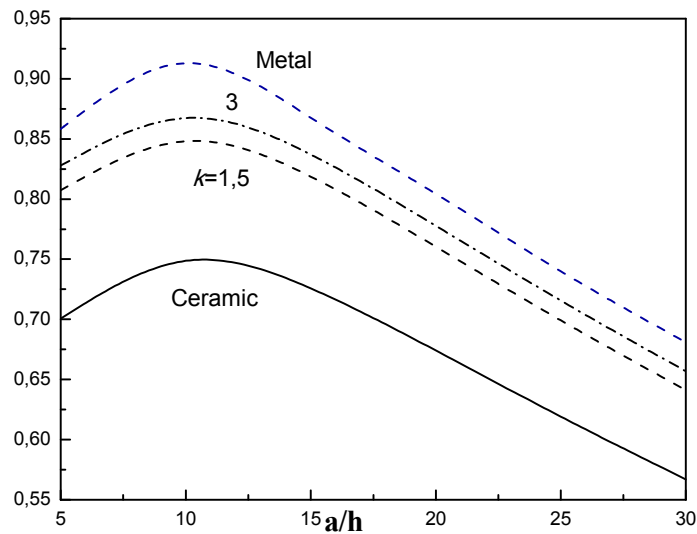


Fig. 5 Dimensionless center deflection as a function of side-to-thickness ratio a/h for a FG sandwich square plates ($t_{FGM} = 0.2h, t_1 = 0, q_0 = t_2 = t_3 = 100$).

Figs. 6 and 7 show the through-the-thickness distributions of the non-dimensional axial stress $\bar{\sigma}_x$ and the transverse shear stress $\bar{\tau}_{xz}$ of the FG sandwich plate for $k = 3$ and $t_{FGM} = 0.2h$, respectively. Distinction between the curves in Figs. 6 and 7 is obvious which demonstrate the great effect played by the different thermal and bending loads on the axial and transverse shear stresses.

Fig. 8 shows the through-the-thickness distribution of axial stress $\bar{\sigma}_x$ of the homogeneous

ceramic and FG sandwich plates. The stresses are tensile below the mid-plane and compressive above the mid-plane. As expected, the different volume fraction exponent influences considerably the distribution of axial stresses.

Fig. 9 presents the through-the-thickness distribution of the transverse shear stress $\bar{\tau}_{xz}$ for $k = 0, 0.5, 1, \text{ and } 3$. The maximum value occurs at a point on the mid-plane of the plate and its magnitude for FG plate is larger than that for homogeneous ceramic plate.

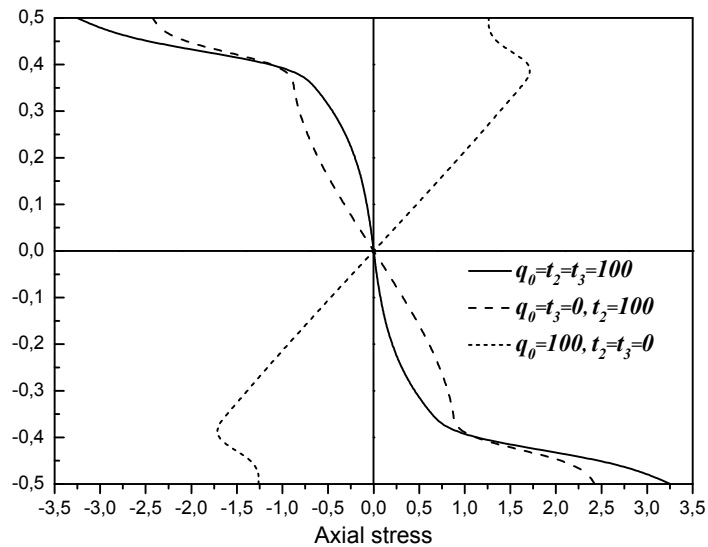


Fig. 6 Effect of mechanical and temperature loads on the dimensionless axial stress $\bar{\sigma}_x$ of FG sandwich plate ($t_{FGM} = 0.2h, k = 3$)

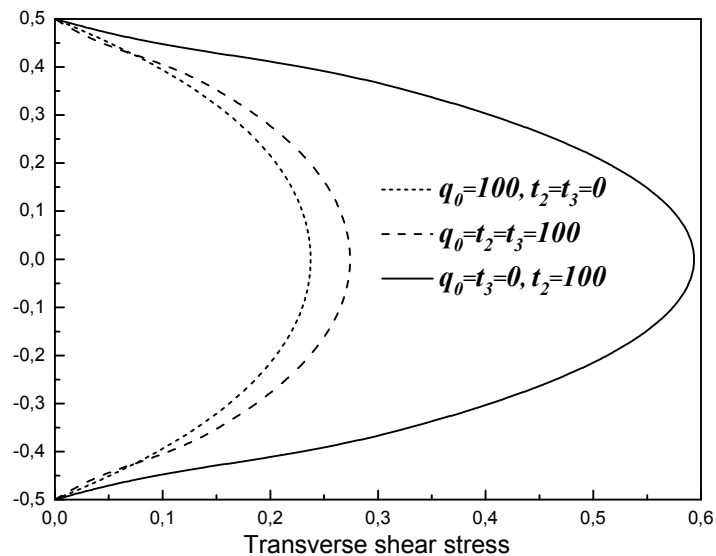


Fig. 7 Effect of mechanical and temperature loads on the dimensionless transverse shear stress $\bar{\tau}_{xz}$ of FG sandwich plate ($t_{FGM} = 0.2h, k = 3$)

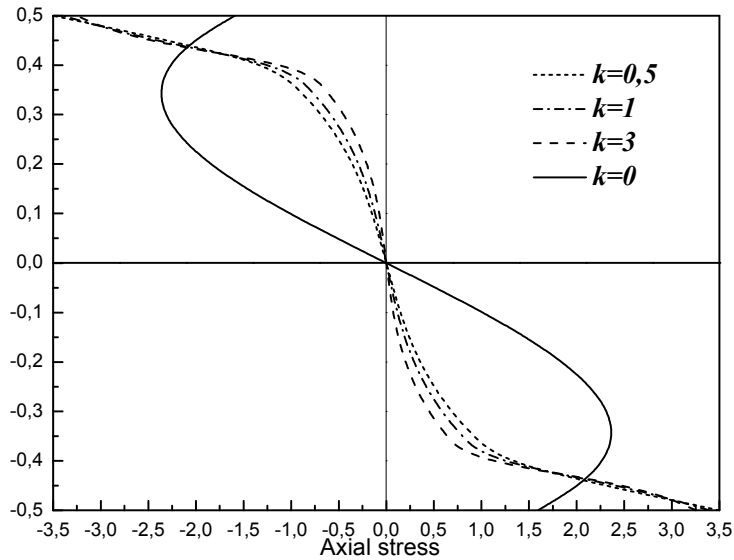


Fig. 8 Variation of axial stress $\bar{\sigma}_x$ through the plate thickness for FG sandwich plates ($t_{FGM} = 0.2h$, $t_0 = 0, q_0 = t_2 = t_3 = 100$)

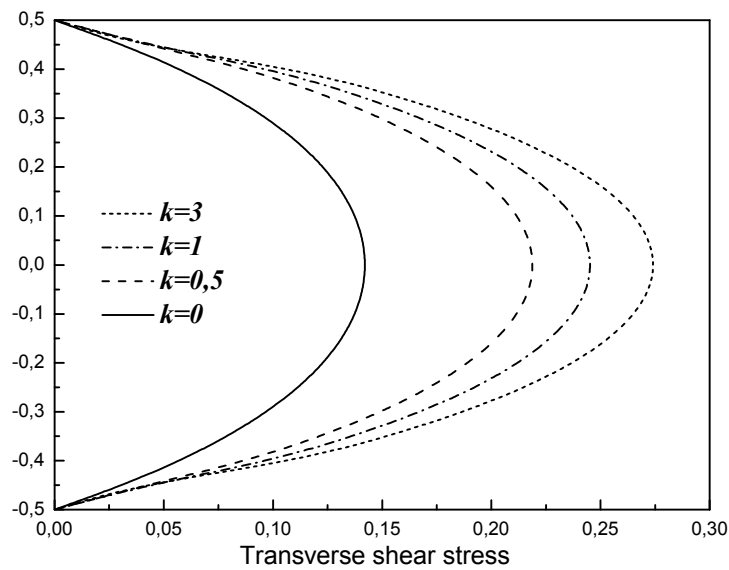


Fig. 9 Variation of transverse shear stress $\bar{\sigma}_x$ through the plate thickness for FG sandwich plates ($t_{FGM} = 0.2h, t_0 = 0, q_0 = t_2 = t_3 = 100$)

5. Conclusions

This work presents a thermomechanical bending analysis for FG sandwich plates using an original quasi-3D HSDT with 5 unknowns. The theory considers the stretching and shear deformation effects without requiring a shear correction factor. The gradation of mechanical

properties within the thickness is supposed to be of the power law type and comparisons have been made with homogeneous isotropic plates. Comparison studies have been performed to describe the efficiency of the present theory. Indeed, we strongly propose applying the present theory because it contains a special kinematic with smaller number of variables than the classical FSDT and other HSDTs. Numerical results for different volume fraction indices, thickness ratios, temperature rise have been presented. It is concluded that the gradation in the material properties and the temperature field have a considerable influence on the thermomechanical bending response of the FG sandwich plates.

References

- Ait Amar Meziane, M., Abdelaziz, H.H. and Tounsi, A. (2014), "An efficient and simple refined theory for buckling and free vibration of exponentially graded sandwich plates under various boundary conditions", *J. Sandw. Struct. Mater.*, **16**(3), 293-318.
- Ait Yahia, S., Ait Atmane, H., Houari, M.S.A. and Tounsi, A. (2015), "Wave propagation in functionally graded plates with porosities using various higher-order shear deformation plate theories", *Struct. Eng. Mech., Int. J.*, **53**(6), 1143-1165.
- Attia, A., Tounsi, A., Adda Bedia, E.A. and Mahmoud, S.R. (2015), "Free vibration analysis of functionally graded plates with temperature-dependent properties using various four variable refined plate theories", *Steel Compos. Struct., Int. J.*, **18**(1), 187-212.
- Belabed, Z., Houari, M.S.A., Tounsi, A., Mahmoud, S.R. and Anwar Bég, O. (2014), "An efficient and simple higher order shear and normal deformation theory for functionally graded material (FGM) plates", *Composites: Part B*, **60**, 274-283.
- Bellifa, H., Benrahou, K.H., Hadji, L., Houari, M.S.A. and Tounsi, A. (2016), "Bending and free vibration analysis of functionally graded plates using a simple shear deformation theory and the concept the neutral surface position", *J. Braz. Soc. Mech. Sci. Eng.*, **38**(1), 265-275.
- Bennoun, M., Houari, M.S.A. and Tounsi, A. (2016), "A novel five variable refined plate theory for vibration analysis of functionally graded sandwich plates", *Mech. Adv. Mater. Struct.*, **23**(4), 423-431.
- Bessaim, A., Houari, M.S.A., Tounsi, A., Mahmoud, S.R. and Adda Bedia, E.A. (2013), "A new higher-order shear and normal deformation theory for the static and free vibration analysis of sandwich plates with functionally graded isotropic face sheets", *J. Sandw. Struct. Mater.*, **15**(6), 671-703.
- Bouchafa, A., Bachir Bouiadjra, M., Houari, M.S.A. and Tounsi, A. (2015), "Thermal stresses and deflections of functionally graded sandwich plates using a new refined hyperbolic shear deformation theory", *Steel Compos. Struct., Int. J.*, **18**(6), 1493-1515.
- Bouderba, B., Houari, M.S.A. and Tounsi, A. (2013), "Thermomechanical bending response of FGM thick plates resting on Winkler–Pasternak elastic foundations", *Steel Compos. Struct., Int. J.*, **14**(1), 85-104.
- Bouguenina, O., Belakhdar, K., Tounsi, A. and Adda Bedia, E.A. (2015), "Numerical analysis of FGM plates with variable thickness subjected to thermal buckling", *Steel Compos. Struct., Int. J.*, **19**(3), 679-695.
- Bounouara, F., Benrahou, K.H., Belkorissat, I. and Tounsi, A. (2016), "A nonlocal zeroth-order shear deformation theory for free vibration of functionally graded nanoscale plates resting on elastic foundation", *Steel Compos. Struct., Int. J.*, **20**(2), 227-249.
- Bourada, M., Kaci, A., Houari, M.S.A. and Tounsi, A. (2015), "A new simple shear and normal deformations theory for functionally graded beams", *Steel Compos. Struct., Int. J.*, **18**(2), 409-423.
- Bourada, F., Amara, K. and Tounsi, A. (2016), "Buckling analysis of isotropic and orthotropic plates using a novel four variable refined plate theory", *Steel Compos. Struct., Int. J.*, **21**(6), 1287-1306.
- Bousahla, A.A., Houari, M.S.A., Tounsi, A. and Adda Bedia, E.A. (2014), "A novel higher order shear and normal deformation theory based on neutral surface position for bending analysis of advanced composite plates", *Int. J. Computat. Methods*, **11**(6), 1350082.

- Carrera, E., Brischetto, S., Cinefra, M. and Soave, M. (2011), "Effects of thickness stretching in functionally graded plates and shells", *Composites: Part B*, **42**(2), 123-133.
- Cetkovic, M. and Vuksanovic, D.J. (2000), "Bending, free vibrations and buckling of laminated composite and sandwich plates using a layerwise displacement model", *Compos. Struct.*, **88**(2), 219-227.
- Dutta, G., Panda, S.K., Mahapatra, T.R. and Singh, V.K. (2016), "Electro-magneto-elastic response of laminated composite plate: A finite element approach", *Int. J. Appl. Computat. Math.*, 1-20.
- Golmakani, M.E. (2013), "Large deflection thermoelastic analysis of shear deformable functionally graded variable thickness rotating disk", *Composites: Part B*, **45**(1), 1143-1155.
- Grover, N., Maiti, D.K. and Singh, B.N. (2013), "A new inverse hyperbolic shear deformation theory for static and buckling analysis of laminated composite and sandwich plates", *Compos. Struct.*, **95**, 667-675.
- Hamidi, A., Houari, M.S.A., Mahmoud, S.R. and Tounsi, A. (2015), "A sinusoidal plate theory with 5-unknowns and stretching effect for thermomechanical bending of functionally graded sandwich plates", *Steel Compos. Struct., Int. J.*, **18**(1), 235-253.
- Hebali, H., Tounsi, A., Houari, M.S.A., Bessaim, A. and Adda Bedia, E.A. (2014), "A new quasi-3D hyperbolic shear deformation theory for the static and free vibration analysis of functionally graded plates", *ASCE J. Eng. Mech.*, **140**(2), 374-383.
- Houari, M.S.A., Tounsi, A. and Anwar Bég, O. (2013), "Thermoelastic bending analysis of functionally graded sandwich plates using a new higher order shear and normal deformation theory", *Int. J. Mech. Sci.*, **76**, 102-111.
- Houari, M.S.A., Tounsi, A., Bessaim, A. and Mahmoud, S.R. (2016), "A new simple three-unknown sinusoidal shear deformation theory for functionally graded plates", *Steel Compos. Struct., Int. J.*, **22**(2), 257-276.
- Kar, V.R. and Panda, S.K. (2015a), "Large deformation bending analysis of functionally graded spherical shell using FEM", *Struct. Eng. Mech., Int. J.*, **53**(4), 661-679.
- Kar, V.R. and Panda, S.K. (2015b), "Nonlinear flexural vibration of shear deformable functionally graded spherical shell panel", *Steel Compos. Struct., Int. J.*, **18**(3), 693-709.
- Kar, V.R. and Panda, S.K. (2016), "Nonlinear thermomechanical behaviour of FGM cylindrical / hyperbolic / elliptical shell panel with TD and TID properties", *J. Press. Vessel Technol. ASME*, **138**(6), 061206.
- Kar, V.R. and Panda, S.K. (2016), "Nonlinear thermomechanical deformation behaviour of P-FGM shallow spherical shell panel", *Chinese J. Aeronaut.*, **29**(1), 173-183.
- Kar, V.R., Mahapatra, T.R. and Panda, S.K. (2015), "Nonlinear flexural analysis of laminated composite flat panel under hygro-thermo-mechanical loading", *Steel Compos. Struct., Int. J.*, **19**(4), 1011-1033.
- Koiter, W.T. (1959), "A consistent first approximation in the general theory of thin elastic shells", *Proceedings of 1st Symposium on the Theory of Thin Elastic Shells*, Amsterdam, North-Holland.
- Larbi Chaht, F., Kaci, A., Houari, M.S.A., Tounsi, A., Anwar Bég, O. and Mahmoud, S.R. (2015), "Bending and buckling analyses of functionally graded material (FGM) size-dependent nanoscale beams including the thickness stretching effect", *Steel Compos. Struct., Int. J.*, **18**(2), 425-442.
- Mahapatra, R., Panda, S.K. and Kar, V.R. (2016a), "Nonlinear flexural analysis of laminated composite panel under hygro-thermo-mechanical loading – A micromechanical approach", *Int. J. Computat. Methods*, **13**(3), 1650015(1-33).
- Mahapatra, T.R., Kar, V.R. and Panda, V.R. (2016b), "Large amplitude bending behaviour of laminated composite curved panels", *Eng. Computat.*, **33**(1), 116-138.
- Mahi, A., Adda Bedia, E.A. and Tounsi, A. (2015), "A new hyperbolic shear deformation theory for bending and free vibration analysis of isotropic, functionally graded, sandwich and laminated composite plates", *Appl. Math. Model.*, **39**(9), 2489-2508.
- Matsunaga, H. (2009), "Stress analysis of functionally graded plates subjected to thermal and mechanical loadings", *Compos. Struct.*, **87**(4), 344-357.
- Mehar, K. and Panda, S.K. (2016), "Thermoelastic analysis of FG-CNT reinforced shear deformable composite plate under various loading", *Int. J. Computat. Methods*, 1750019.
- Natarajan, S. and Manickam, G. (2012), "Bending and vibration of functionally graded material sandwich plates using an accurate theory", *Finite Elem. Anal. Des.*, **57**, 32-42.

- Nguyen, T.K. (2015), "A higher-order hyperbolic shear deformation plate model for analysis of functionally graded materials", *Int. J. Mech. Mater. Des.*, **11**(2), 203-219.
- Reddy, J.N. and Cheng, Z.Q. (2001), "Three-dimensional thermomechanical deformations of functionally graded rectangular plates", *Euro. J. Mech. A Solids*, **20**(5), 841-855.
- Sahoo, S.S., Panda, S.K., Singh, V.K. (2015), "Experimental and numerical investigation of static and free vibration responses of woven Glass/Epoxy laminated composite plate", *Proceedings of IMechE Part L: Journal of Materials: Design and Applications*, 1464420715600191.
- Sahoo, S.S., Panda, S.K. and Mahapatra, T.R. (2016a), "Static, free vibration and transient response of laminated composite curved shallow panel – An experimental approach", *Euro. J. Mech.-A/Solids*, **59**, 95-113.
- Sahoo, S.S., Singh, V.K. and Panda, S.K. (2016b), "Nonlinear flexural analysis of shallow laminated carbon/epoxy composite curved shell panels: Experimental and numerical investigation", *J. Eng. Mech. ASCE*, **142**(4).
- Saidi, H., Houari, M.S.A., Tounsi, A. and Adda Bedia, E.A. (2013), "Thermo-mechanical bending response with stretching effect of functionally graded sandwich plates using a novel shear deformation theory", *Steel Compos. Struct., Int. J.*, **15**(2), 221-245.
- Shariyat, M. (2010), "A generalized high-order global–local plate theory for nonlinear bending and buckling analyses of imperfect sandwich plates subjected to thermo-mechanical loads", *Compos. Struct.*, **92**(1), 130-143.
- Singh, V.K., Mahapatra, T.R. and Panda, S.K. (2016), "Nonlinear flexural analysis of single/doubly curved smart composite shell panels integrated with PFRC actuator", *Euro. J. Mech.-A/Solids*, **60**, 300-314.
- Sobhy, M. (2013), "Buckling and free vibration of exponentially graded sandwich plates resting on elastic foundations under various boundary conditions", *Compos. Struct.*, **99**, 76-87.
- Talha, M. and Singh, B.N. (2011), "Thermo-mechanical induced vibration characteristics of shear deformable functionally graded ceramic-metal plates using the finite element method", *Proceedings of the Institution of Mechanical Engineers, Part C: Journal of Mechanical Engineering Science*, **225**, 50-65.
- Tounsi, A., Houari, M.S.A., Benyoucef, S. and Adda Bedia, E.A. (2013), "A refined trigonometric shear deformation theory for thermoelastic bending of functionally graded sandwich plates", *Aerosp. Sci. Technol.*, **24**(1), 209-220.
- Tounsi, A., Houari, M.S.A. and Bessaim, A. (2016), "A new 3-unknowns non-polynomial plate theory for buckling and vibration of functionally graded sandwich plate", *Struct. Eng. Mech., Int. J.*, **60**(4), 547-565.
- Xiang, S., Wang, K., Ai, Y., Sha, Y. and Shi, H. (2009), "Analysis of isotropic, sandwich and laminated plates by a meshless method and various shear deformation theories", *Compos. Struct.*, **91**(1), 31-37.
- Zenkour, A.M. and Alghamdi, N.A. (2008), "Thermoelastic bending analysis of functionally graded sandwich plates", *J. Mater. Sci.*, **43**(8), 2574-2589.
- Zidi, M., Tounsi, A., Houari, M.S.A., Adda Bedia, E.A. and Anwar Bég, O. (2014), "Bending analysis of FGM plates under hygro-thermo-mechanical loading using a four variable refined plate theory", *Aerosp. Sci. Technol.*, **34**, 24-34.